




# Senecavirus-Specific Recombination Assays Reveal the Intimate Link between Polymerase Fidelity and RNA Recombination

Chen Li,<sup>a</sup> Haiwei Wang,<sup>a</sup> Jiabao Shi,<sup>a</sup> Decheng Yang,<sup>a</sup> Guohui Zhou,<sup>a</sup> Jitao Chang,<sup>a</sup> Craig E. Cameron,<sup>b</sup>  Andrew Woodman,<sup>b</sup> Li Yu<sup>a</sup>

<sup>a</sup>Division of Livestock Infectious Diseases, State Key Laboratory of Veterinary Biotechnology, Harbin Veterinary Research Institute, Chinese Academy of Agricultural Sciences, Harbin, People's Republic of China

<sup>b</sup>Department of Biochemistry & Molecular Biology, The Pennsylvania State University, University Park, Pennsylvania, USA

**ABSTRACT** Senecavirus A (SVA) is a reemerging virus, and recent evidence has emphasized the importance of SVA recombination *in vivo* on virus evolution. In this study, we report the development of an infectious cDNA clone for the SVA/HLJ/CHA/2016 strain. We used this strain to develop a reporter virus expressing enhanced green fluorescent protein (eGFP), which we then used to screen for a recombination-deficient SVA by an eGFP retention assay. Sequencing of the virus that retained the eGFP following passage allowed us to identify the nonsynonymous mutations (S460L alone and I212V-S460L in combination) in the RNA-dependent RNA polymerase (RdRp) region of the genome. We developed a Senecavirus-specific cell culture-based recombination assay, which we used to elucidate the role of RdRp in SVA recombination. Our results demonstrate that these two polymerase variants (S460L and I212V/S460L) have reduced recombination capacity. These results indicate that the RdRp plays a central role in SVA replicative recombination. Notably, our results showed that the two recombination-deficient variants have higher replication fidelity than the wild type (WT) and display decreased ribavirin sensitivity compared to the WT. In addition, these two mutants exhibited significantly increased fitness *in vitro* compared to the WT. These results demonstrate that recombination and mutation rates are intimately linked. Our results have important implications for understanding the crucial role of the RdRp in virus recombination and fitness, especially in the molecular mechanisms of SVA evolution and pathogenicity.

**IMPORTANCE** Recent evidence has emphasized the importance of SVA recombination on virus evolution *in vivo*. We describe the first assays to study Senecavirus A recombination. The results show that the RNA-dependent RNA polymerase plays a crucial role in recombination and that recombination can impact the fitness of SVA in cell culture. Further, SVA polymerase fidelity is closely related to recombination efficiency. The results provide key insights into the role of recombination in positive-strand RNA viruses.

**KEYWORDS** RNA polymerases, recombination, Senecavirus

Senecavirus A (SVA), formerly known as Seneca Valley virus (SVV), was first reported in 2002 from a PER.C6 cell culture and belongs to the genus *Senecavirus* within the family *Picornaviridae* (1). The virus has been sporadically circulating in pig herds in the United States since the late 1980s. However, cases of SVA-associated vesicular disease were reported in Canada in 2007 and in the United States in 2012 (2). After 2014, a sudden increase in outbreaks of SVA affecting pigs was documented in Brazil, China, Thailand, Colombia, and Vietnam (3–6), suggesting that the disease has become a worldwide problem (7). The genome of SVA is a single-stranded positive-sense RNA

**Citation** Li C, Wang H, Shi J, Yang D, Zhou G, Chang J, Cameron CE, Woodman A, Yu L. 2019. Senecavirus-specific recombination assays reveal the intimate link between polymerase fidelity and RNA recombination. *J Virol* 93:e00576-19. <https://doi.org/10.1128/JVI.00576-19>.

**Editor** Julie K. Pfeiffer, University of Texas Southwestern Medical Center

**Copyright** © 2019 American Society for Microbiology. All Rights Reserved.

Address correspondence to Andrew Woodman, [auw23@psu.edu](mailto:auw23@psu.edu), or Li Yu, [yuli02@caas.cn](mailto:yuli02@caas.cn).

C.L. and H.W. contributed equally to this work.

**Received** 5 April 2019

**Accepted** 5 April 2019

**Accepted manuscript posted online** 17 April 2019

**Published** 14 June 2019

that is ~7,300 nucleotides (nt) in length. The genome organization is similar to that of other picornaviruses, which have a large single open reading frame (ORF) flanked by highly structured 5' and 3' untranslated regions (UTRs) encompassing *cis*-acting elements essential for viral transcription, translation, and replication (1). The ORF is translated into a single polyprotein that is posttranslationally processed by the three viral proteases Lpro, 2A, and 3C into the protein products P1 (VP4, VP2, VP3, and VP1), P2 (2A, 2B, and 2C), and P3 (3A, 3B, 3Cpro, and 3D<sup>pol</sup>) (1).

It is well established that the abundant genetic diversity observed in many RNA viruses has important consequences for viral pathogenesis, host tropism, and evolution (8, 9). Two predominant mechanisms contribute to the variability of RNA viruses, the error-prone RNA-dependent RNA polymerase (RdRp) that lacks proofreading ability, leading to high mutation rates (10–12), and recombination, where chimeric viruses can be generated following coinfection of the same cell by two closely related viruses (13–15). Indeed, recombination is proposed to be a key evolutionary mechanism in RNA viruses that is required to purge the genome of deleterious mutations that accumulate following error-prone replication (15, 16). From a public health perspective, it is known that the recombination process has important implications, as it is associated with the reemergence of new antigenic variants and the generation of new virus strains (9, 12, 17–19). For example, the live attenuated Sabin vaccine strain is known to recombine with cocirculating species C enterovirus, where subsequent infection can lead to pathogenic outcomes (20, 21). Further, intrahost recombination events in the related foot-and-mouth disease virus (FMDV) play a significant role in increasing genetic diversity in FMDV quasispecies (22–24). However, much less recombination is observed when virus infection occurs in multiple wildlife species in southern Africa (25), while recombination seems to dominate when FMDV infection occurs in a very narrow host range (23).

Mutation and recombination are essential for RNA virus adaptation and evolution (26–29). Both are primarily mediated by the RdRp, as indicated by recent studies of recombination in enteroviruses and alphaviruses (30–32). Indeed, these recent studies strongly indicate that polymerase fidelity is also associated with virus recombination efficiency. For example, Sindbis virus, with a low-fidelity RdRp, is prone to recombine, which results in the overproduction of defective interfering particles (31). In addition, modification of polymerase fidelity impacted the rate of recombination in poliovirus (32). Alternatively, studies in poliovirus have shown that recombination is necessary for virus entry into the central nervous system, and recombination could elevate adaptation without changing the optimal mutation rate (19). These observations led us to investigate the role RdRp played in SVA recombination. To date, it is reported that pigs are the only natural SVA host, and SVA recombination has been reported (33). In addition, a second study identified an 11-nucleotide insertion in the 5' UTR region of the SVV GD04/2017 strain (34). Both examples emphasize the currently poorly understood role of SVA recombination *in vivo*.

We hypothesized that we could select for RdRp variants that may reduce SVA recombination. In this study, SVA recombination-defective variants were isolated by using an eGFP retention assay, analogous to one reported by the Andino laboratory that used poliovirus as a model (19). Two variants that were further examined had amino acid changes to the RdRp, S460L alone, and I212V-S460L in combination. To characterize the impact of these RdRp mutants on virus recombination, we developed the first reported SVA-specific recombination assay, based upon previous cell-based approaches used for enteroviruses (30, 32, 35, 36). The SVA-S460L and SVA-I212V-S460L variants were shown to be replication competent but recombination defective. The defect in recombination was replication independent. Importantly, further investigation showed that both variants have increased polymerase fidelity. Further, both of the isolated recombination-deficient variants showed higher fitness than did the SVA wild type (WT) in competition studies in cell culture. These findings and the results within show that the RdRp and fidelity play a crucial role in the recombination and fitness of SVA in cell culture.

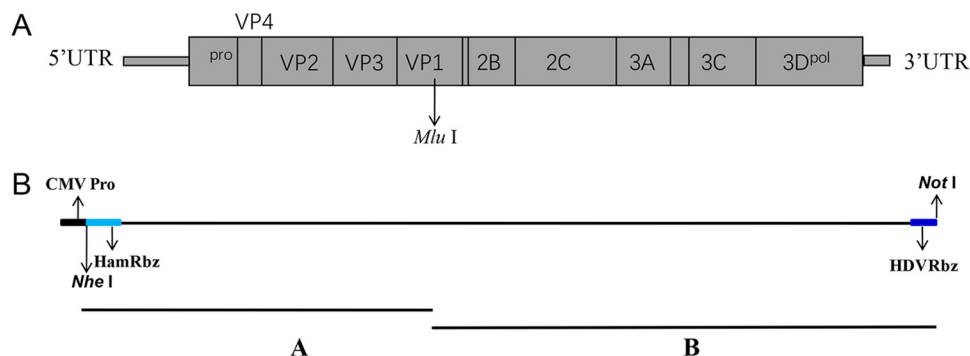


**FIG 1** Schematic diagram of the full-length SVA genome and construction of the full-length cDNA clones. (A) Genome organization of SVA. The ORFs are flanked by 5' and 3' UTRs, followed by the poly(A) tail at the 3' end. The arrow showing a mutation at nucleotide G3305T to activate the MluI restriction enzyme site in cloned virus in panel B. (B) Two separate genomic fragments were synthesized and assembled into the PCI vector using the unique restriction enzyme sites. The full-length viral genome is under the control of a CMV promoter and followed by a hammerhead ribozyme.

## RESULTS

**Generation of an infectious clone of SVA strain SVA/HLJ/CHA/2016.** The full-length genome of SVA/HLJ/CHA/2016 strain was sequenced (GenBank accession number [KY419132](#)), as described previously (4). The overall strategy to construct the infectious clone of the SVA strain SVA/HLJ/CHA/2016 is shown in Fig. 1A and B. Fragments A and B were synthesized and assembled (see Materials and Methods). The full-length genome sequence of SVA was then engineered into the PCI vector, producing the pSVA16 clone.

To rescue the SVA virus, the plasmid pSVA16 was transfected into BHK-21 cells. After 48 hours, the BHK-21 cells displayed typical cytopathic effect (CPE) compared with the negative-control groups (blank) (Fig. 2A). The cells and transfection supernatants were then harvested and subjected to an immunofluorescence assay using polyclonal antibodies against SVA capsid protein. A strong positive signal can be detected in the cells infected with the infectious clone of SVA, indicating that the SVA virus was successfully rescued from the BHK-21 cells (Fig. 2B). The average virus titer and one-step growth curves indicated that the 10th passage of rescued SVA had similar replication kinetics to its parental virus passaged in BHK-21 cells (Fig. 2C and D). Further, the morphology of SVA particles was determined by phosphotungstate negative staining. Electron microscopic observation revealed that the particles were spherical, with a diameter of 30 nm (Fig. 2E). Compared to the genome sequence of the parental virus, the DNA sequence of pSVA16 contained a mutation at nucleotide 3305, G3305T, to activate the MluI restriction enzyme site in the 2C region for differentiating the cloned virus from the parental virus. The G3305T mutation is a silent mutation with no change to the encoded amino acid sequence or impact on virus replication (Fig. 2C and D).

**Isolation of recombination-deficient SVA mutants.** To identify virus determinants that modulate the recombination rate of SVA, we constructed a genetic system composed of a replication-competent enhanced green fluorescent protein (eGFP)-expressing virus. The recombinant SVA that encodes eGFP within the viral polyprotein was constructed as described previously (37), with minor modifications. Here, the eGFP is flanked by a cotranslational “ribosome skipping” FMDV 2A (F2A) (38) (Fig. 3A). Typically, reporter-expressing viruses are known to be unstable and lose the nonvirus sequence by a recombination mechanism (19). We used this knowledge to identify recombination-deficient SVA mutants that retain the eGFP reporter signal following serial passage, performed in a manner analogous to that shown for poliovirus (15). Chimeric viruses were cloned by limiting dilution and screened for eGFP expression, as described previously (19) (Fig. 3B). The clones expressing eGFP were isolated and further propagated. This cycle was repeated until the ratio of eGFP-positive to CPE-positive wells was greater than 0.7.

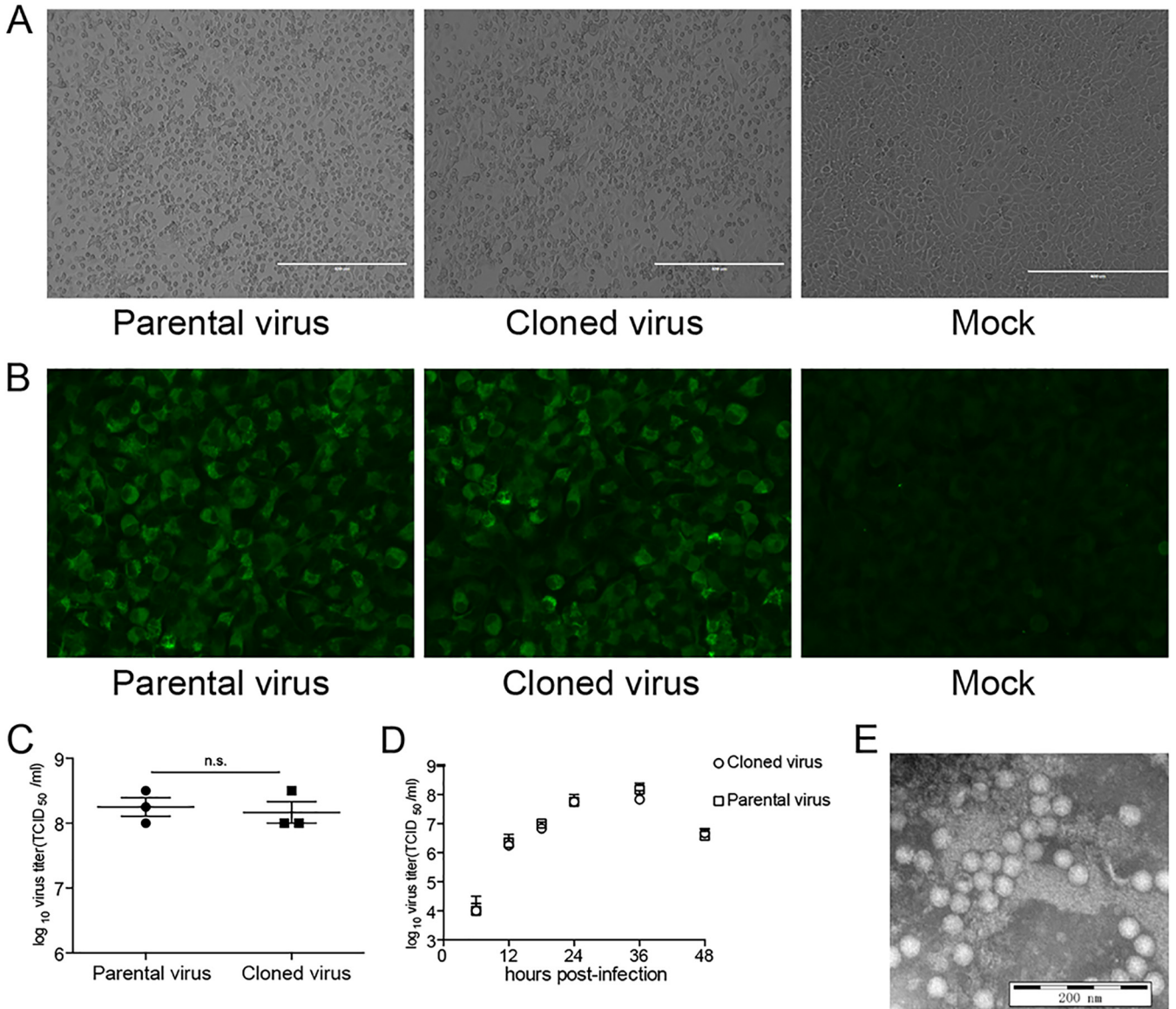


**FIG 2** Generation of an infectious clone of SVA/HLJ/CHA/2016. (A) CPE of the parental and cloned viruses in BHK-21 cells, mock control without virus infection. (B) Immunofluorescence assay of the parental and cloned viruses in BHK-21 cells and mock control without virus infection. (C) Growth characteristics of the parental and cloned viruses in BHK-21 cells. The viruses were passaged 10 times in BHK-21 cells, and the titers of progeny viruses were determined by a TCID<sub>50</sub> assay. The standard deviations ( $n = 3$ ) of mean virus titers are shown. n.s., nonsignificant. (D) Replication ability of the parental and cloned virus. BHK-21 cells were infected with the parental or cloned viruses at an MOI of 0.01. The virus harvested at different times was titrated and expressed as the TCID<sub>50</sub>. The mean  $\pm$  standard deviation (SD) values are shown (repeated-measures ANOVA,  $n = 3$ ). (E) Electron micrograph visualization of cloned viruses. Scale bar = 200 nm.

After selection, the supernatants of the wells that were positive for eGFP expression were sequenced by TA cloning. All 10 cloned viruses that were selected had nonsynonymous mutations to the 3D<sup>P<sub>ol</sub></sup>. Nine of the 10 viruses contained the serine-to-leucine substitution at nucleotide 460 (Table 1). In addition, three of the isolates contained a substitution of valine to alanine at nucleotide 218, isoleucine to valine at nucleotide 212, or histidine to arginine at nucleotide 79 (Table 1). These observations strongly suggested that one or more of these substitutions negatively impacted the recombination rate of the SVA. Interestingly, the S460L, I212V, and V218A mutations were located in regions of the RdRp that would be near the RNA channel of the polymerase. In contrast, the H79R mutation appears to be located on the surface of the RdRp and away from any region that would interact with the viral RNA (Fig. 3C). To validate our observations, the identified mutations were introduced into the SVA-eGFP infectious

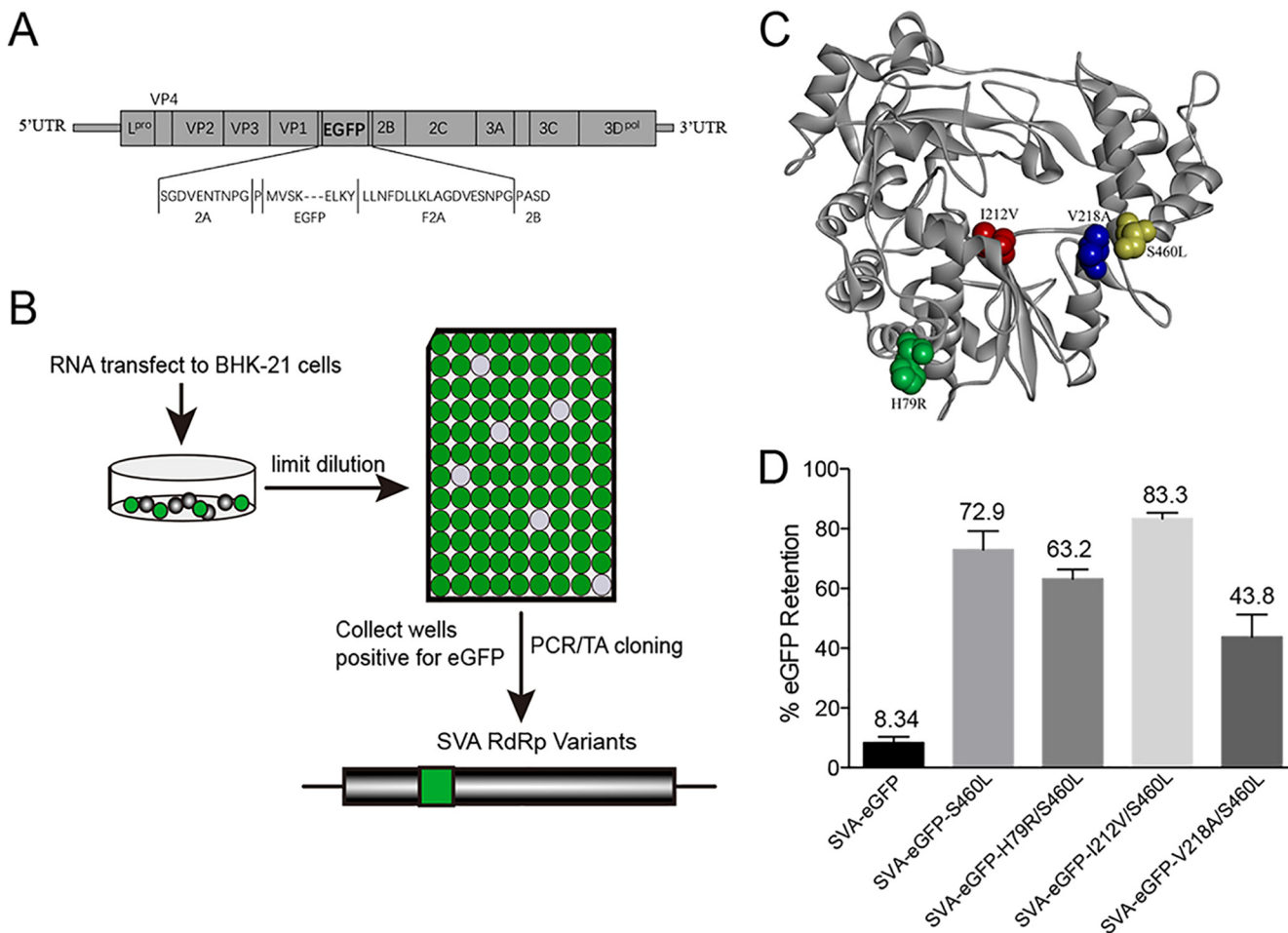


**FIG 3** Isolation of recombination-deficient SVA variants. (A) A scheme of the reporter virus genome with an eGFP-F2A fusion gene inserted between 2A and 2B. F2A, foot-and-mouth disease virus 2A peptide. (B) The gene of eGFP was cloned into SVA genome. The resulting recombinant virus was used to infect BHK-21 cells, and eGFP retention was measured between passages by limiting dilution. Two mutations, I212V and S460L, within 3D<sup>pol</sup> confer an increase in eGFP retention. (C) The structure of RNA-dependent RNA polymerase of the SVA. Colors show locations of mutations affecting recombination, as follows: yellow, S460L; red, I212V; blue, V218A; green, H79R. (D) eGFP retention of SVA and SVA mutants was measured by limiting dilution in BHK-21 cells. SVA-eGFP, SVA-eGFP-S460L, SVA-eGFP-V218A/S460L, SVA-eGFP-I212V-S460L, and SVA-eGFP-H79R/S460L were passaged five times in BHK-21 cells with the eGFP ratio quantified. Mean ± SD values are shown (repeated-measures ANOVA, *n* = 3).

clone individually or in combination to test for eGFP retention. All variants were infectious and were designated SVA-eGFP-S460L, SVA-eGFP-V218A-S460L, SVA-eGFP-I212V-S460L, and SVA-eGFP-H79R-S460L. Compared to wild-type eGFP-expressing virus at passage 5, SVA-eGFP-S460L showed a significant increase, to ~70%, in the eGFP-positive proportion. The SVA-eGFP-I212V-S460L double mutant showed a further increase

**TABLE 1** Mutations identified in the 3D polymerase regions of the SVA in passage 10

Clone	Mutation in 3D polymerase regions of viral population				
	H79R	V94A	I212V	V218A	S460L
M1				X	X
M2		X			X
M3			X		X
M4					X
M5					X
M6					X
M7					X
M8	X				X
M9					X
M10					X

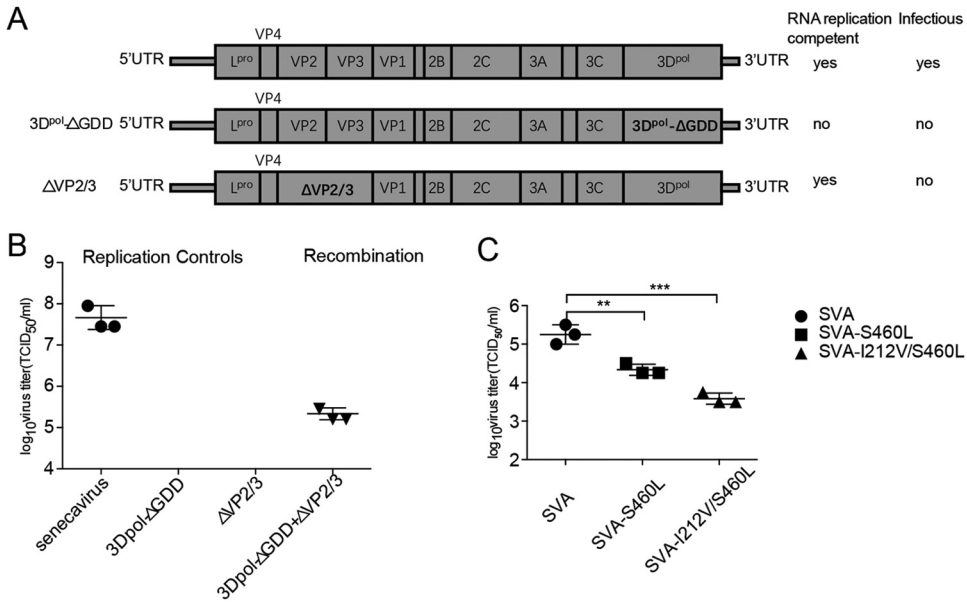


**FIG 4** Replicative RNA recombination of SVA variants. (A) Schematic of the viral RNAs used in the SVA recombination assay. Their genotypic and phenotypic differences are depicted. A lethal GDD deletion in the 3D<sup>pol</sup> active site and a lethal capsid deletion make them noninfectious, only a recombination event between the two following cotransfection will produce viable progeny (B) Yields of virus produced in Ad293 cells. Cells were transfected with individual viral RNAs (replication controls) or two noninfectious RNAs (recombination). The titers of progeny viruses were determined by a TCID<sub>50</sub> assay. The standard deviations (*n* = 3) of mean virus titers are shown. (C) Frequencies of RNA recombination in Ad293 cells cotransfected with capsid donor containing 3D<sup>pol</sup> mutations and 3D<sup>pol</sup> ΔGDD RNAs. The titers of progeny viruses were determined by a TCID<sub>50</sub> assay. The standard deviations (*n* = 3) of mean virus titers are shown (Student's *t* test, *n* = 3; \*\*, *P* < 0.01; \*\*\*, *P* < 0.001).

in the eGFP-positive proportion, to ~80%, indicating that I212V had an additive effect. In contrast, the SVA-eGFP-H79R-S460L and SVA-eGFP-V218A-S460L mutants showed a decrease in the eGFP-positive ratio compared to that with S460L mutation alone (Fig. 3D). Based upon these observations, the S460L and I212V-S460L mutants were chosen from this screen for further investigation.

**Recombination rates of SVA-S460L and SVA-I212V-S460L mutants are significantly decreased.** Based on previous studies of recombination in enteroviruses (35, 36), a cell culture-based recombination assay was developed and performed to further examine the effect of S460L and I212V-S460L on SVA replicative RNA recombination. This assay utilized the two following parental viral RNAs that are independently unable to generate viable progeny: SVA-3D<sup>pol</sup>ΔGDD, where the deletion of three amino acids from the 3D<sup>pol</sup> active site renders the polymerase inactive so no replication can occur; and SVA-ΔVP2/3, a replicon that does not encode areas of the structural proteins rendering the SVA RNA noninfectious (Fig. 4A). Only following cotransfection of the two noninfectious RNAs can recombination be observed. Single transfections produced no virus, as expected (Fig. 4A and B). We subsequently introduced the S460L and I212V-S460L mutations into the SVA-ΔVP2/3 template and carried out a cotransfection. Following incubation, recombinant virus was isolated and the titer determined (see Materials and Methods). Our data showed that introduction of the S460L and I212V-S460L mutations into the 3D<sup>pol</sup> of SVA-ΔVP2/3 significantly reduced the number of viable recombinant progeny compared to the wild type by 5.62- and 31.62-fold, respectively (Fig. 4C). This result strongly suggested that the two mutations had an additive effect upon recombination in support of our observations in the eGFP retention assay.

**Recombination-defective variants show a high-fidelity phenotype with reduced ribavirin sensitivity.** Mutations in the viral polymerase are known to influence fidelity and have been associated with the rate of recombination (28, 32, 39). We therefore set out to determine if the fidelity of SVA-S460L and SVA-I212V-S460L were different from

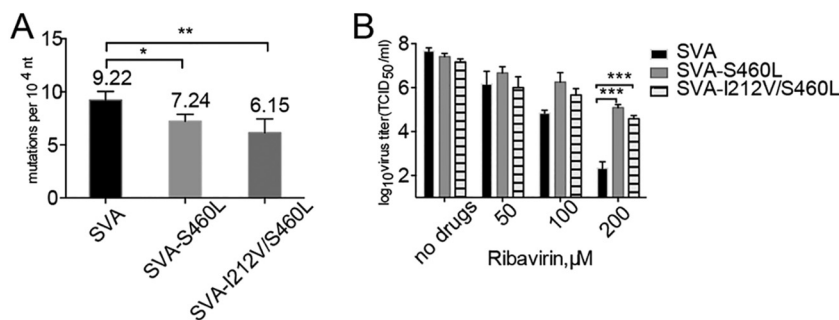


**FIG 5** Recombination-defective variants show a high-fidelity phenotype. (A) A mean of 70 partial P1 sequences (approximately 35,000 nucleotides per replicate) were obtained. The mean mutation frequencies (number of nucleotide mutations per 10,000 nt sequenced)  $\pm$  SD represent all replicates. The same pattern of reduced mutation frequency for other polymerase mutants compared to the WT was observed for each replicate (two-tailed Mann-Whitney test,  $n = 3$ ; \*,  $P < 0.05$ ; \*\*,  $P < 0.01$ ). (B) RNA virus mutagen sensitivity assay of viral strains. BHK-21 cells, treated with different concentrations of ribavirin or mock treated, were infected at an MOI of 0.01; at 72 h postinfection, the infectivity in the progeny virus was determined by TCID<sub>50</sub> assay. Mean  $\pm$  SD virus titers are shown (Student's  $t$  test,  $n = 4$ ; \*\*\*,  $P < 0.001$ ).

that of the WT. We sequenced an area of the P1 coding region to determine the relative frequency of mutation (see Materials and Methods). Our data show that the SVA-S460L and SVA-I212V-S460L mutants produced significantly fewer mutations than does the WT, with fidelity increased by 1.27- and 1.50-fold, respectively (Fig. 5A). Previous studies have shown that enhanced polymerase fidelity confers resistance to mutagens (40–42). To further confirm viral replication fidelity, we evaluated the sensitivity of each mutant to ribavirin. The results showed that the SVA-S460L and SVA-I212V-S460L mutants were significantly less sensitive than the WT when exposed to a 200  $\mu$ M concentration of ribavirin (Fig. 5B). Together, these results demonstrated that SVA-S460L and SVA-I212V-S460L are high-fidelity mutants. As the recombination rates of the two mutants were significantly different from that of the WT, we interpret that SVA fidelity and recombination rate are linked, and the extent of reduction of recombination rate correlates positively with replication fidelity.

#### Recombination-defective virus does not exhibit reduced fitness in cell culture.

We examined the growth characteristics of SVA-S460L and SVA-I212V-S460L over a single replication cycle in BHK-21 and PK-15 cells. In BHK-21 and PK-15 cells, no significant differences in the production of infectious particles were observed between each mutant and the WT. In addition to infectious virus yield, we quantified total genomic RNA by real-time PCR. The two polymerase mutants and the WT virus produced similar levels of RNA in the two cell types (Fig. 6A and B). Together, these results indicate that the mutations had no impact on virus replication. To assess whether the substitutions result in a subtle fitness change for the variants *in vitro*, a comparison of fitness between the SVA-S460L, SVA-I212V-S460L, and SVA WT was performed via competition assays in both BHK-21 and PK-15 cells. In direct competition assays (Fig. 6C), after three successive passages, the 460L chromatogram peaks were higher than the 460S peaks, and the 212V chromatogram peaks were higher than the 212I peaks, indicating that the recombination-deficient variants had a fitness advantage over the SVA WT in both types of cells when competed. However, the fitness of SVA-I212V-S460L is slightly lower than that of the SVA-S460L in BHK-21 cells. Taken together, these results indicated that recombination-defective variants do not hamper virus replication in BHK-21 cells culture and the recombination-defective variants are able to outcompete the SVA WT in both types of cells.

## DISCUSSION

Recombination is an event that occurs during virus replication that in some circumstances generates chimeric viruses that are more fit than either parental strains (15). SVA is a reemerging virus, and recombinant forms of SVA are known to appear in nature (33). In this study, we established a reverse genetics system for an SVA strain,

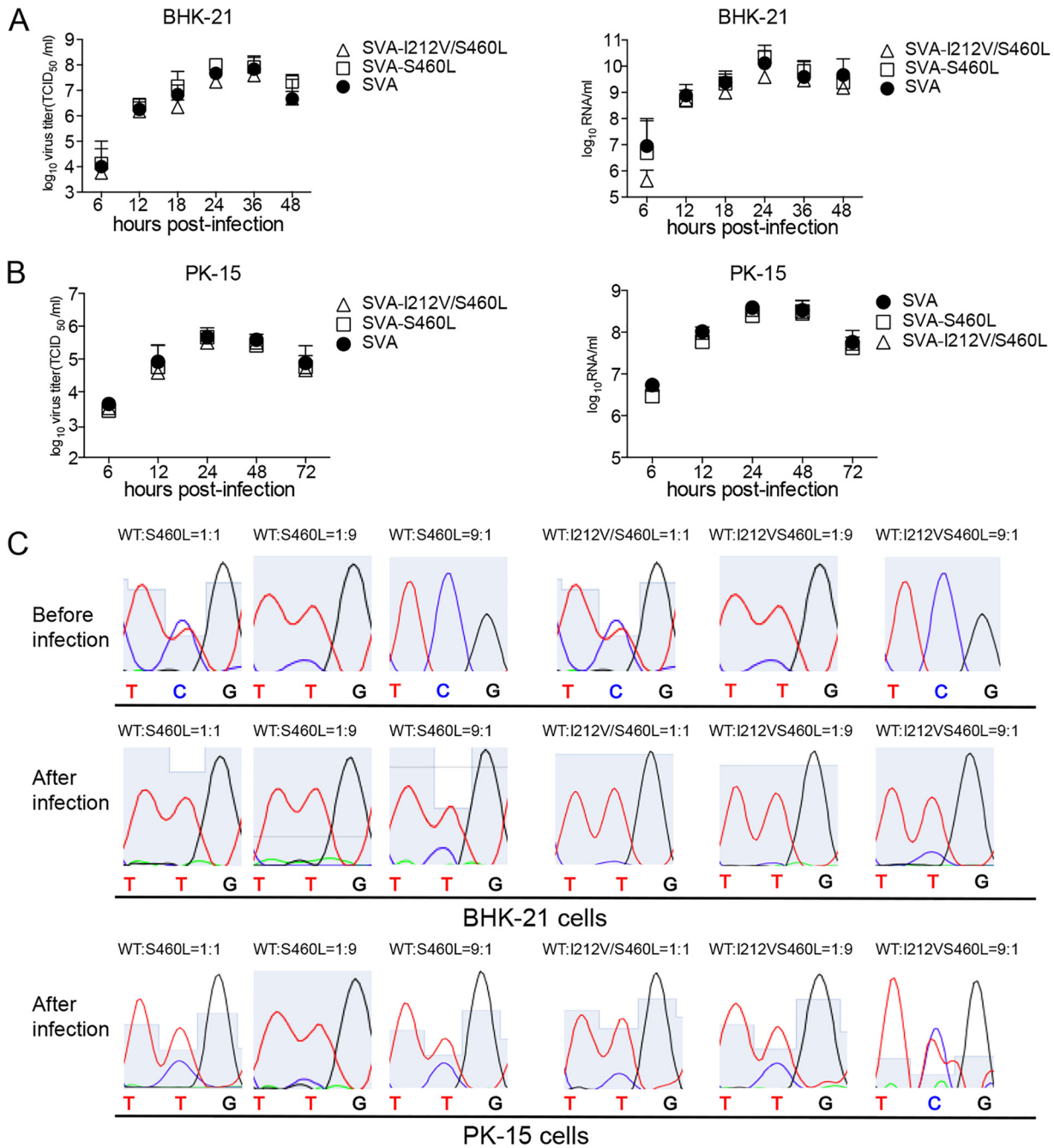


**FIG 6** Recombination-deficient mutations do not exhibit reduced fitness in cell culture. (A and B) Replication ability of SVA high-fidelity mutants. BHK-21 cells and PK-15 cells were infected with the mutants or SVA WT at an MOI of 0.01. The virus harvested at different times was titrated and expressed as the TCID<sub>50</sub>, and the genome copy numbers were measured for the same samples by real-time reverse transcription-PCR (RT-PCR). Mean ± SD values are shown (repeated-measures ANOVA, *n* = 3; ns for all mutants compared with WT). (C) The SVA-S460L or SVA-I212V-S460L mutant was mixed with the WT at a ratio of 9:1, 1:1, or 1:9 to inoculate BHK-21 cells at an MOI of 0.1 for three passages, after which the 3D<sup>Pro</sup> region was sequenced. The abundance of each competitor was measured as the height of the nucleotide peak for the mutant (T nt) or the WT (C nt) in sequencing chromatograms.

SVA/HLJ/CHA/2016, that has emerged in China. More importantly, by the development of two recombination-specific assays, we have identified two important residues in the SVA RdRp that decreased the efficiency of viral RNA recombination. Our data further show that these two SVA recombination-defective variants are high-fidelity mutants. Furthermore, the polymerase mutations that reduce recombination render the virus more resistance to the antiviral drug ribavirin. Our data strongly support the interpretation that polymerase fidelity and replicative recombination efficiency are linked.



In principle, recombination can occur in all RNA viruses and in many cases is not site specific, suggesting that there are either different mechanisms for this process or strong selection pressures for proteome functionality after recombination has occurred (36). For mechanisms of viral RNA recombination, two major models have been suggested. The commonly accepted replicative model involves template switching of the viral RdRp during negative-strand RNA synthesis, also known as copy-choice recombination (19, 36, 43–45). The nonreplicative model involves breakage and rejoining of viral RNA, albeit at a much lower frequency than with copy-choice recombination (28, 46–48). By using an eGFP retention assay, similar to that of Xiao et al., who used PV as a model (19), we were able to identify nonsynonymous mutations to the SVA RdRp. Further characterization showed that two of the variants identified (S460L and I212V-S460L) did significantly increase the level of eGFP retention following serial passage. This strongly suggested that these mutations inhibited the template-switching event(s) that occur to remove the nonviral gene by homologous recombination. The cell culture-based recombination-specific assay that we developed was also based upon the successful assays developed for PV and enterovirus A71 (EV-A71) (31–33, 35). When we introduced the two identified mutations, we showed that the replicative RNA recombination rates of SVA-S460L and SVA-I212V-S460L were significantly decreased compared to that of the WT. Unlike the observations of Xiao et al., we show that these variants were of higher fidelity than the WT (Fig. 5A). The high-fidelity SVA-I212V-S460L variant led to an approximately 31.62-fold decrease in recombinant yield, suggestive that for SVA, a high-fidelity polymerase decreases the rate of template switching, a result in agreement with studies in PV and other RNA virus species groups, like the *Togaviridae* and *Orthomyxoviridae* (32, 36, 49).

Recombination is proposed to be crucial for viruses to build up beneficial mutations and suppress deleterious mutations that may occur during error-prone replication (16). This ensures that the viruses take maximal advantage of a few beneficial mutations without being overwhelmed by an accumulation of deleterious mutations. All of this is dependent on the interplay between mutation rate and recombination (50). Since recombination and mutation rate seem to be functionally linked, it was interesting to see that the high-fidelity SVA-S460L and SVA-I212V-S460L mutants showed slightly increased fitness when competed against WT. This was consistent in two different cell lines. It would seem that, in cell culture at least, those viruses that are reduced/unable to recombine may have a subtle growth advantage. This phenomenon has also been observed in PV, where a recombination-deficient virus outcompeted the WT in cell culture but was attenuated *in vivo* (51). Acevedo et al. reported that the bottlenecks that are observed *in vivo* seem to be far more severe than in the cell culture plate and may explain the need for recombination in the wild (51). Indeed, previous studies have shown that the diversity of the quasispecies is essential for viruses adapting to and surviving new selective pressures in changing environments (11, 52–54). These reports, along with this study reinforce the idea that in addition to RdRp fidelity, the interplay between recombination and mutation rate are connected to virus fitness. In further support of this, a previous study has shown that the FMDV high-fidelity variant R84H has increased fitness *in vitro*, but the virus with this mutation showed an attenuated phenotype (55, 56). Work is ongoing to characterize whether the recombination-deficient variants in this study could be attenuated in pigs.

Previous cell-based assays for recombination have suggested that recombination may be a biphasic replicative process involving the generation of greater-than genome length for poliovirus and coxsackievirus B3 (CVB3) (32, 36, 57). The subsequent deletion of genome duplications generated recombinants of the correct genome length. Interestingly, recombinants containing sequence duplications have been observed from *in vivo* samples of a bovine viral diarrhea virus (BVDV)-infected animal (58). These results indicated that an initial recombination event with cellular RNA sequences takes place, confirming that the generation of imprecise recombinants may be a natural step of the recombination process. Recently, we developed a serum-free BHK-21 cell suspension culture platform for the production of an inactivated SVA vaccine. However, exogenous

sequence insertion was observed for FMDV-infected suspension cells, suggesting that promiscuous recombination between the FMDV genome and host cell mRNA produced the recombinant virus (59). Here, the SVA recombination-deficient virus variant could be considered for a suitable vaccine seed virus to reduce the possibility of virus recombination with cellular sequence.

In summary, we have developed two recombination-specific assays for SVA and explored the modulation of SVA recombination and its correlation with mutation rate and fitness. Our results fit with the majority of current observations found in many RNA virus groups and further support the recently observed phenomenon that RdRp fidelity and template-switching efficiency are linked. The results provide key insights into the role of recombination in the evolutionary dynamics of RNA viruses, and the assays developed here can be used by the scientific community to understand the mechanisms of this biologically and economically important process.

## MATERIALS AND METHODS

**Cells and viruses.** BHK-21 (baby hamster kidney cell line) cells were grown in Dulbecco's modified Eagle's medium (DMEM; Gibco) supplemented with 10% fetal bovine serum (FBS; HyClone Laboratories, Inc., South Logan, UT) and 1% penicillin-streptomycin at 37°C in 5% CO<sub>2</sub>. The wild-type SVA/HLJ/CHA/2016 virus (GenBank accession number [KY419132](#)) was obtained from finishing pigs on a farm in Heilongjiang Province in northeast China in 2016, as described previously (4). The isolated virus was cultured on BHK-21 cells.

**Plasmid construction.** In order to construct a full-length cDNA clone, the 5'-end genomic sequence of SVA/HLJ/CHA/2016 was further determined using a 5'-rapid amplification of cDNA ends (5'-RACE) PCR, followed by TA cloning. Here, a full-length SVA/HLJ/CHA/2016 genomic cDNA clone was constructed using the strategy shown in Fig. 1B. A hammerhead ribozyme sequence (HamRbz; 5'-TGT TAA GCG TCT GAT GAG TCC GTG AGG ACG AAA CTA TAG GAA AGG AAT TCC TAT AGT C-3') was inserted upstream of fragment A, while a hepatitis D virus (HDV) ribozyme element (5'-GGG TCG GCA TGG CAT CTC CAC CTC CTC GCG GTC CGA CCT GGG CAT CCG AAG GAG GAC GCA CGT CCA CTC GGA TGG CTA AGG GAG GGC G-3') was fused to the 3' terminus of the viral genome (fragment B) to create synthetic runoff transcripts that contained a 3' terminus identical to that of the viral RNA. The two separate fragments under the control of the eukaryotic RNA polymerase II (Pol II) cytomegalovirus (CMV) promoter were chemically synthesized at Tsingke Biological Technology Company and assembled. To create a molecular marker for differentiating cloned virus from the parental virus SVA/HLJ/CHA/2016, a MluI restriction endonuclease site was introduced with a G3305T synonymous mutation (Fig. 1A). The full-length cDNA clone of SVA/HLJ/CHA/2016 was assembled and cloned into vector PCI, and the resulting full-length cDNA clone was designated pSVA16 (Fig. 1B). To construct a full-length cDNA clone expressing eGFP, the eGFP gene fused with a foot-and-mouth disease virus 2A element (F2A) at its C terminus. The eGFP-F2A fusion gene was inserted between the SVA genes 2A and 2B using overlap extension PCR method (60). This full-length cDNA clone was designated pSVA-eGFP (Fig. 1C).

A 9-base deletion in 3D<sup>pol</sup> (<sup>6825</sup>GGU GAC GAC<sup>6833</sup>) was engineered using site-directed mutagenesis, resulting in a RNA replication-incompetent derivative of SVA (Fig. 4A, pSVA-3DpolΔGDD). An in-frame deletion of VP2 and VP3 capsid gene sequences (nucleotides [nt] 1119 to 2687) was used to make an RNA replication-competent subgenomic replicon (Fig. 4A, pSVA-ΔVP2/3). 3D<sup>pol</sup> substitution mutations (SVA-S460L and SVA-I212V-S460L) were engineered into full-length infectious pSVA16 and pSVA-ΔVP2/3 cDNA clones.

**Recovery of recombinant viruses.** BHK-21 cells seeded in 6-well plate were transfected with pSVA16, pSVA-S460L, and pSVA-I212V-S460L. Transfection was conducted using the Lipofectamine 3000 reagent, following the manufacturer's instructions (Life Technologies, NY, USA). Cytopathic effect (CPE) was monitored daily after infection. Recombinant viruses were harvested when significant CPE was observed. The recovered viruses were passaged 10 times in BHK-21 cells, and the stability of the introduced mutations was confirmed by sequencing of the 3D<sup>pol</sup>-coding region.

**Indirect immunofluorescence assay.** BHK-21 cells in 96-well plates were infected with SVA, fixed with ice-cold anhydrous ethanol for 15 min at 4°C, and air-dried. Fixed cells were treated with 50 μl/well of the SVA-positive serum from pig at a 1:200 dilution in phosphate-buffered saline (PBS) and incubated for 1 h at 37°C. After washing with PBS, 50 μl/well of fluorescein isothiocyanate (FITC)-conjugated goat anti-pig IgG (Sigma, St. Louis, MO, USA) at a 1:200 dilution was added and incubated for 1 h at 37°C. Plates were washed three times with PBS and examined under an Olympus microscope connected to a Leica DFC490 digital color camera.

**Virus purification and transmission electron microscopy.** BHK-21 cells infected with the rescued SVA were collected and subjected to three freeze-thaw cycles. Cellular debris was removed by centrifugation at 6,000 × g for 30 min at room temperature. The pH of the supernatant was adjusted to 7.4, and the virus was precipitated with 8% polyethylene glycol 8000 (PEG 8000) and 0.3 M NaCl for 16 h at 4°C while constantly rotating. Precipitated virus was centrifuged at 6,000 × g for 30 min at room temperature. Subsequently, the resuspended pellet in TNE buffer (50 mM Tris, 10 mM NaCl, EDTA, 1 mM [pH 7.6]) was centrifuged through 30% sucrose cushion in NTE buffer at 100,000 × g for 120 min in an SW41 rotor. The pellet was resuspended in 100 μl of TNE buffer. The purified virus was negatively stained.

Transmission electron microscopy images were collected with a JEM-1200EX transmission electron microscope.

**TCID<sub>50</sub> assay and growth curve.** Tenfold serial dilutions of virus were prepared in 96-well round-bottom plates in DMEM. Dilutions were performed in octuplicate, and 50  $\mu$ l of the dilution was transferred to 10<sup>4</sup> BHK-21 cells plated in 100  $\mu$ l of DMEM with 2% FBS. After 3 days, 50% tissue culture infective dose (TCID<sub>50</sub>) values were determined by the Reed-Muench formula (61).

To determine viral replication kinetics, growth experiments in BHK-21 cells were performed as follows. First, cell monolayers in 6-well tissue culture plates were washed with phosphate-buffered saline (PBS) and inoculated with different viruses at a multiplicity of infection (MOI; equal to PFU number/cell) of 0.01. The plates were incubated for 1 h at 37°C. Then, the cells were washed three times with PBS to remove unbound virus particles and covered with DMEM supplemented with 2% FBS. The infected cells were incubated at 37°C and harvested at different times. The plates were subjected to three consecutive freeze-thaw cycles, and cell debris was removed by centrifugation. The viral titers of the supernatants were determined by a TCID<sub>50</sub> assay. Mean values and standard deviations were calculated from the results from three independent experiments.

**Selection of recombination-deficient virus.** Titers of SVA-eGFP in BHK-21 cells in an initial viral stock were determined and expressed as a TCID<sub>50</sub>. Plates were scanned on an EnSpire multimode plate reader using the following settings: measurement mode, fluorescence bottom; excitation wavelength, 475 nm; emission wavelength, 512 nm; plate type, 96 wells; measurement height, 9.5 nm; number of flashes, 500. Supernatant from wells positive for eGFP was collected, combined, and then the titer determined by TCID<sub>50</sub>. This cycle was repeated until the ratio of eGFP-positive to CPE-positive wells was greater than 0.7. SVA RNA was extracted using a Simply P total RNA extraction kit (BioFlux, Hangzhou, China), and cDNA was generated by reverse transcription of total RNA using PrimeScript reverse transcriptase (TaKaRa, Dalian, China). To identify recombination-deficient SVA variants, the 3D<sup>pol</sup>-coding region was amplified by PCR with the Easy-A high-fidelity PCR cloning enzyme (Stratagene, Foster City, CA). The PCR product was purified and cloned into the pMD18-T vector (TaKaRa) for sequencing. The sequencing data were analyzed using the Lasergene software package (DNASTar, Inc., Madison, WI). Variants fixed in this population were recloned into the SVA-eGFP vector, *in vitro* transcribed, and then transfected into BHK-21 cells. To measure the rate of retention of eGFP, virus from these cells was diluted into 96-well plates at 0.25 TCID<sub>50</sub> per well, and fluorescence and CPE were monitored (19).

**Cell-based recombination assay.** *In vitro*-transcribed RNA from either pSVA-3Dpol $\Delta$ GDD plus pSVA- $\Delta$ VP2/3 or pSVA-3Dpol $\Delta$ GDD plus pSVA- $\Delta$ VP2/3-S460L or pSVA-3Dpol $\Delta$ GDD plus pSVA- $\Delta$ VP2/3-I212V/S460L was cotransfected (500 ng each per well in a 6-well plate) into Ad293 cells using the Lipofectamine 3000 reagent, following the manufacturer's instructions (Life Technologies, NY, USA), as described previously (35). Plates were harvested at 72 h posttransfection, and virus was recovered after three rounds of freezing and thawing and cleared of cellular debris by centrifugation at 3,000 rpm. Recombinant virus in the supernatant was quantified by the TCID<sub>50</sub> in BHK-21 cells.

**Sequencing for mutational frequency.** SVA RNA was extracted using a Simply P Total RNA extraction kit (BioFlux, Hangzhou, China), and cDNA was generated by reverse transcription of the total RNA using PrimeScript reverse transcriptase (TaKaRa, Dalian, China). To determine mutation frequencies, a part of the P1 structural gene was amplified by PCR with the Easy-A high-fidelity PCR cloning enzyme (Stratagene, Foster City, CA). The PCR product was purified and cloned into the pMD18-T vector (TaKaRa) for sequencing. The sequencing data were analyzed using the Lasergene software package (DNASTar, Inc., Madison, WI). The number of mutations per 10<sup>4</sup> nucleotides sequenced was determined as the total number of mutations identified in each population divided by the total number of nucleotides sequenced for that population multiplied by 10<sup>4</sup>. For each population, 60 to 80 partial P1 structural gene sequences of approximately 500 nt per replicate (primers flanking genome positions 2800 to 3300) were sequenced. Mutation frequencies (mutations per 10,000 nt) were determined as described previously (62).

**RNA mutagen assays.** BHK-21 cell monolayers were pretreated with various concentrations of ribavirin or 5-fluorouracil (5-FU; Sigma, USA) for 3 h. These mutagen concentrations were not highly toxic to the cells over the 72-h incubation period. The cells were infected with the rescued SVA variants at an MOI of 0.01 for 1 h and were subsequently treated with the same mutagen concentration as that during the pretreatment. The infected cell cultures were then incubated at 37°C in 5% CO<sub>2</sub> for 72 h. For the final stage of the experiment, virus was released from the cells by three cycles of freeze-thaw, and the lysate was clarified by centrifugation at 6,500  $\times$  g for 5 min. The titer of the lysate was determined using a TCID<sub>50</sub> assay on BHK-21 cells. Mean values and standard deviations were calculated from the results from three independent experiments.

**Direct competition fitness assay.** For the direct competition fitness assay, each of the rescued SVA mutants was mixed with its parent virus at a ratio of 9:1, 1:1, or 1:9 to infect BHK-21 cells in triplicate wells at an MOI of 0.1 over three passages. Viral RNA was extracted, and the region corresponding to the 3D<sup>pol</sup> gene was amplified by reverse transcription-PCR (RT-PCR) for sequencing. The abundance of each competitor was measured as the height of the peak for the nucleotide corresponding to the WT or mutant sequence in the sequencing chromatogram.

**Statistical analysis.** The mutation frequency was evaluated using a two-tailed paired *t* test. The growth curves and RNA synthesis profiles of each mutant and SVA WT were compared using repeated-measures analysis of variance (ANOVA). Drug resistance was assessed using Student's *t* test. All statistical tests were conducted using the GraphPad Prism software. *P* values of >0.05 were not significant.

## ACKNOWLEDGMENTS

This work was supported by grants from The National Key Research and Development Program of China (grants 2017YFD0501101 and 2016YFD0501505). C.E.C. and A.W. are supported by grant AI45818 from the NIAID, NIH. A.W. is the recipient of a fellowship (18POST33960071) from the American Heart Association (AHA).

## REFERENCES

- Hales LM, Knowles NJ, Reddy PS, Xu L, Hay C, Hallenbeck PL. 2008. Complete genome sequence analysis of Seneca Valley virus-001, a novel oncolytic picornavirus. *J Gen Virol* 89:1265–1275. <https://doi.org/10.1099/vir.0.83570-0>.
- Pasma T, Davidson S, Shaw SL. 2008. Idiopathic vesicular disease in swine in Manitoba. *Can Vet J* 49:84–85.
- Saeng-Chuto K, Stott CJ, Wegner M, Kaewprommal P, Piriyaopansa J, Nilubol D. 2018. The full-length genome characterization, genetic diversity and evolutionary analyses of Senecavirus A isolated in Thailand in 2016. *Infect Genet Evol* 64:32–45. <https://doi.org/10.1016/j.meegid.2018.06.011>.
- Wang H, Li C, Zhao B, Yuan T, Yang D, Zhou G, Yu L. 2017. Complete genome sequence and phylogenetic analysis of Senecavirus A isolated in Northeast China in 2016. *Arch Virol* 162:3173–3176. <https://doi.org/10.1007/s00705-017-3480-4>.
- Zhu Z, Yang F, Chen P, Liu H, Cao W, Zhang K, Liu X, Zheng H. 2017. Emergence of novel Seneca Valley virus strains in China, 2017. *Transbound Emerg Dis* 64:1024–1029. <https://doi.org/10.1111/tbed.12662>.
- Arzt J, Bertram MR, Vu LT, Pauszek SJ, Hartwig EJ, Smoliga GR, Palinski R, Stenfeldt C, Fish IH, Hoang BH, Phuong NT, Hung VV, Vu PP, Dung NK, Dong PV, Tien NN, Dung DH. 2019. First detection and genome sequence of senecavirus A in Vietnam. *Microbiol Resour Announc* 8:e01247-18. <https://doi.org/10.1128/MRA.01247-18>.
- Zhang X, Zhu Z, Yang F, Cao W, Tian H, Zhang K, Zheng H, Liu X. 2018. Review of Seneca Valley virus: a call for increased surveillance and research. *Front Microbiol* 9:940. <https://doi.org/10.3389/fmicb.2018.00940>.
- Elena SF, Sanjuan R. 2005. RNA viruses as complex adaptive systems. *Biosystems* 81:31–41. <https://doi.org/10.1016/j.biosystems.2005.02.001>.
- Holland J, Spindler K, Horodyski F, Grabau E, Nichol S, VandePol S. 1982. Rapid evolution of RNA genomes. *Science* 215:1577–1585. <https://doi.org/10.1126/science.7041255>.
- Domingo E, Holland JJ. 1997. RNA virus mutations and fitness for survival. *Annu Rev Microbiol* 51:151–178. <https://doi.org/10.1146/annurev.micro.51.1.151>.
- Domingo E, Escarmis C, Sevilla N, Moya A, Elena SF, Quer J, Novella IS, Holland JJ. 1996. Basic concepts in RNA virus evolution. *FASEB J* 10:859–864. <https://doi.org/10.1096/fasebj.10.8.8666162>.
- Lam TT, Zhu H, Guan Y, Holmes EC. 2016. Genomic analysis of the emergence, evolution, and spread of human respiratory RNA viruses. *Annu Rev Genomics Hum Genet* 17:193–218. <https://doi.org/10.1146/annurev-genom-083115-022628>.
- Ledinko N. 1963. Genetic recombination with poliovirus type 1. Studies of crosses between a normal horse serum-resistant mutant and several guanidine-resistant mutants of the same strain. *Virology* 20:107–119. [https://doi.org/10.1016/0042-6822\(63\)90145-4](https://doi.org/10.1016/0042-6822(63)90145-4).
- Lai MM. 1992. RNA recombination in animal and plant viruses. *Microbiol Rev* 56:61–79.
- Simon-Loriere E, Holmes EC. 2011. Why do RNA viruses recombine? *Nat Rev Microbiol* 9:617–626. <https://doi.org/10.1038/nrmicro2614>.
- Oberste MS, Penaranda S, Pallansch MA. 2004. RNA recombination plays a major role in genomic change during circulation of coxsackie B viruses. *J Virol* 78:2948–2955. <https://doi.org/10.1128/JVI.78.6.2948-2955.2004>.
- Becher P, Orlich M, Thiel HJ. 2001. RNA recombination between persisting pestivirus and a vaccine strain: generation of cytopathogenic virus and induction of lethal disease. *J Virol* 75:6256–6264. <https://doi.org/10.1128/JVI.75.14.6256-6264.2001>.
- Jarvis TC, Kirkegaard K. 1992. Poliovirus RNA recombination: mechanistic studies in the absence of selection. *EMBO J* 11:3135–3145. <https://doi.org/10.1002/j.1460-2075.1992.tb05386.x>.
- Xiao Y, Rouzine IM, Bianco S, Acevedo A, Goldstein EF, Farkov M, Brodsky L, Andino R. 2017. RNA recombination enhances adaptability and is required for virus spread and virulence. *Cell Host Microbe* 22:420. <https://doi.org/10.1016/j.chom.2017.08.006>.
- Kew O, Morris-Glasgow V, Landaverde M, Burns C, Shaw J, Garib Z, Andre J, Blackman E, Freeman CJ, Jorba J, Sutter R, Tambini G, Venczel L, Pedreira C, Laender F, Shimizu H, Yoneyama T, Miyamura T, van Der Avoort H, Oberste MS, Kilpatrick D, Cochi S, Pallansch M, de Quadros C. 2002. Outbreak of poliomyelitis in Hispaniola associated with circulating type 1 vaccine-derived poliovirus. *Science* 296:356–359. <https://doi.org/10.1126/science.1068284>.
- Combela N, Holmblat B, Joffret ML, Colbere-Garapin F, Delpeyroux F. 2011. Recombination between poliovirus and coxsackie A viruses of species C: a model of viral genetic plasticity and emergence. *Viruses* 3:1460–1484. <https://doi.org/10.3390/v3081460>.
- Tosh C, Hemadri D, Sanyal A. 2002. Evidence of recombination in the capsid-coding region of type A foot-and-mouth disease virus. *J Gen Virol* 83:2455–2460. <https://doi.org/10.1099/0022-1317-83-10-2455>.
- Ferretti L, Di Nardo A, Singer B, Lasecka-Dykes L, Logan G, Wright CF, Perez-Martin E, King DP, Tuthill TJ, Ribeca P. 2018. Within-host recombination in the foot-and-mouth disease virus genome. *Viruses* 10:E221. <https://doi.org/10.3390/v10050221>.
- Brito B, Pauszek SJ, Hartwig EJ, Smoliga GR, Vu LT, Dong PV, Stenfeldt C, Rodriguez LL, King DP, Knowles NJ, Bachanek-Bankowska K, Long NT, Dung DH, Arzt J. 2018. A traditional evolutionary history of foot-and-mouth disease viruses in Southeast Asia challenged by analyses of non-structural protein coding sequences. *Sci Rep* 8:6472. <https://doi.org/10.1038/s41598-018-24870-6>.
- Lasecka-Dykes L, Wright CF, Di Nardo A, Logan G, Mioulet V, Jackson T, Tuthill TJ, Knowles NJ, King DP. 2018. Full genome sequencing reveals new southern African territories genotypes bringing us closer to understanding true variability of foot-and-mouth disease virus in Africa. *Viruses* 10:E192. <https://doi.org/10.3390/v10040192>.
- Rawson JMO, Nikolaitchik OA, Keele BF, Pathak VK, Hu WS. 2018. Recombination is required for efficient HIV-1 replication and the maintenance of viral genome integrity. *Nucleic Acids Res* 46:10535–10545. <https://doi.org/10.1093/nar/gky910>.
- Aaziz R, Tepfer M. 1999. Recombination in RNA viruses and in virus-resistant transgenic plants. *J Gen Virol* 80:1339–1346. <https://doi.org/10.1099/0022-1317-80-6-1339>.
- Gallei A, Pankraz A, Thiel HJ, Becher P. 2004. RNA recombination in vivo in the absence of viral replication. *J Virol* 78:6271–6281. <https://doi.org/10.1128/JVI.78.12.6271-6281.2004>.
- Ludwig-Begall LF, Mauroy A, Thiry E. 2018. Norovirus recombinants: recurrent in the field, recalcitrant in the lab—a scoping review of recombination and recombinant types of noroviruses. *J Gen Virol* 99:970–988. <https://doi.org/10.1099/jgv.0.001103>.
- Woodman A, Lee KM, Janissen R, Gong YN, Dekker N, Shih SR, Cameron CE. 2018. Predicting intraserootypic recombination in enterovirus 71. *J Virol* 93:e02057-18. <https://doi.org/10.1128/JVI.02057-18>.
- Poirier EZ, Mounce BC, Rozen-Gagnon K, Hooikaas PJ, Stapleford KA, Moratorio G, Vignuzzi M. 2015. Low-fidelity polymerases of alphaviruses recombine at higher rates to overproduce defective interfering particles. *J Virol* 90:2446–2454. <https://doi.org/10.1128/JVI.02921-15>.
- Woodman A, Arnold JJ, Cameron CE, Evans DJ. 2016. Biochemical and genetic analysis of the role of the viral polymerase in enterovirus recombination. *Nucleic Acids Res* 44:6883–6895. <https://doi.org/10.1093/nar/gkw567>.
- Wang Z, Zhang X, Yan R, Yang P, Wu Y, Yang D, Bian C, Zhao J. 2018. Emergence of a novel recombinant Seneca Valley virus in Central China, 2018. *Emerg Microbes Infect* 7:180. <https://doi.org/10.1038/s41426-018-0183-1>.
- Wang M, Chen L, Pan S, Mou C, Shi K, Chen Z. 2019. Molecular evolution and characterization of novel Seneca Valley virus (SVV) strains in South

- China. *Infect Genet Evol* 69:1. <https://doi.org/10.1016/j.meegid.2019.01.004>.
35. Kempf BJ, Peersen OB, Barton DJ. 2016. Poliovirus polymerase Leu420 facilitates RNA recombination and ribavirin resistance. *J Virol* 90: 8410–8421. <https://doi.org/10.1128/JVI.00078-16>.
  36. Lowry K, Woodman A, Cook J, Evans DJ. 2014. Recombination in enteroviruses is a biphasic replicative process involving the generation of greater-than genome length 'imprecise' intermediates. *PLoS Pathog* 10:e1004191. <https://doi.org/10.1371/journal.ppat.1004191>.
  37. Chen Z, Yuan F, Li Y, Shang P, Schroeder R, Lechtenberg K, Henningson J, Hause B, Bai J, Rowland RRR, Clavijo A, Fang Y. 2016. Construction and characterization of a full-length cDNA infectious clone of emerging porcine senecavirus A. *Virology* 497:111–124. <https://doi.org/10.1016/j.virol.2016.07.003>.
  38. Sharma P, Yan F, Doronina VA, Escuin-Ordinas H, Ryan MD, Brown JD. 2012. 2A peptides provide distinct solutions to driving stop-carry on translational recoding. *Nucleic Acids Res* 40:3143–3151. <https://doi.org/10.1093/nar/gkr1176>.
  39. Pfeiffer JK, Kirkegaard K. 2003. A single mutation in poliovirus RNA-dependent RNA polymerase confers resistance to mutagenic nucleotide analogs via increased fidelity. *Proc Natl Acad Sci U S A* 100:7289–7294. <https://doi.org/10.1073/pnas.1232294100>.
  40. Coffey LL, Beeharry Y, Borderia AV, Blanc H, Vignuzzi M. 2011. Arbovirus high fidelity variant loses fitness in mosquitoes and mice. *Proc Natl Acad Sci U S A* 108:16038–16043. <https://doi.org/10.1073/pnas.1111650108>.
  41. Levi LI, Gnädig NF, Beaucourt S, McPherson MJ, Baron B, Arnold JJ, Vignuzzi M. 2010. Fidelity variants of RNA dependent RNA polymerases uncover an indirect, mutagenic activity of amiloride compounds. *PLoS Pathog* 6:e1001163. <https://doi.org/10.1371/journal.ppat.1001163>.
  42. Zeng J, Wang H, Xie X, Li C, Zhou G, Yang D, Yu L. 2014. Ribavirin-resistant variants of foot-and-mouth disease virus: the effect of restricted quasispecies diversity on viral virulence. *J Virol* 88:4008–4020. <https://doi.org/10.1128/JVI.03594-13>.
  43. Kirkegaard K, Baltimore D. 1986. The mechanism of RNA recombination in poliovirus. *Cell* 47:433–443. [https://doi.org/10.1016/0092-8674\(86\)90600-8](https://doi.org/10.1016/0092-8674(86)90600-8).
  44. Arnold JJ, Cameron CE. 1999. Poliovirus RNA-dependent RNA polymerase (3Dpol) is sufficient for template switching in vitro. *J Biol Chem* 274:2706–2716. <https://doi.org/10.1074/jbc.274.5.2706>.
  45. Cheng CP, Nagy PD. 2003. Mechanism of RNA recombination in carmo- and tobusviruses: evidence for template switching by the RNA-dependent RNA polymerase in vitro. *J Virol* 77:12033–12047. <https://doi.org/10.1128/JVI.77.22.12033-12047.2003>.
  46. Gmyl AP, Belousov EV, Maslova SV, Khitrina EV, Chetverin AB, Agol VI. 1999. Nonreplicative RNA recombination in poliovirus. *J Virol* 73: 8958–8965.
  47. Gmyl AP, Korshenko SA, Belousov EV, Khitrina EV, Agol VI. 2003. Non-replicative homologous RNA recombination: promiscuous joining of RNA pieces? *RNA* 9:1221–1231. <https://doi.org/10.1261/rna.5111803>.
  48. Scheel TK, Galli A, Li YP, Mikkelsen LS, Gottwein JM, Bukh J. 2013. Productive homologous and non-homologous recombination of hepatitis C virus in cell culture. *PLoS Pathog* 9:e1003228. <https://doi.org/10.1371/journal.ppat.1003228>.
  49. te Velthuis AJW, Long JC, Bauer DLV, Fan RLY, Yen HL, Sharps J, Siegers JY, Killip MJ, French H, Oliva-Martin MJ, Randall RE, de Wit E, van Riel D, Poon LLM, Fodor E. 2018. Mini viral RNAs act as innate immune agonists during influenza virus infection. *Nat Microbiol* 3:1234–1242. <https://doi.org/10.1038/s41564-018-0240-5>.
  50. Duarte E, Clarke D, Moya A, Domingo E, Holland J. 1992. Rapid fitness losses in mammalian RNA virus clones due to Muller's ratchet. *Proc Natl Acad Sci U S A* 89:6015–6019. <https://doi.org/10.1073/pnas.89.13.6015>.
  51. Acevedo A, Woodman A, Arnold JJ, Yeh MT, Evans DJ, Cameron CE, Andino R. 2018. Genetic recombination of poliovirus facilitates subversion of host barriers to infection. *bioRxiv* <https://doi.org/10.1101/273060>.
  52. Eigen M. 1993. Viral quasispecies. *Sci Am* 269:42–49. <https://doi.org/10.1038/scientificamerican0793-42>.
  53. Vignuzzi M, Stone JK, Arnold JJ, Cameron CE, Andino R. 2006. Quasispecies diversity determines pathogenesis through cooperative interactions within a viral population. *Nature* 439:344–348. <https://doi.org/10.1038/nature04388>.
  54. Andino R, Domingo E. 2015. Viral quasispecies. *Virology* 479–480:46–51. <https://doi.org/10.1016/j.virol.2015.03.022>.
  55. Xin A, Li H, Li L, Liao D, Yang Y, Zhang N, Chen B. 2009. Genome analysis and development of infectious cDNA clone of a virulence-attenuated strain of foot-and-mouth disease virus type Asia 1 from China. *Vet Microbiol* 138:273–280. <https://doi.org/10.1016/j.vetmic.2009.04.009>.
  56. Zeng J, Wang H, Xie X, Yang D, Zhou G, Yu L. 2013. An increased replication fidelity mutant of foot-and-mouth disease virus retains fitness in vitro and virulence in vivo. *Antiviral Res* 100:1–7. <https://doi.org/10.1016/j.antiviral.2013.07.008>.
  57. Holmblat B, Jegouic S, Muslin C, Blondel B, Joffret ML, Delpyroux F. 2014. Nonhomologous recombination between defective poliovirus and coxsackievirus genomes suggests a new model of genetic plasticity for picornaviruses. *mBio* 5:e01119-14. <https://doi.org/10.1128/mBio.01119-14>.
  58. Fricke J, Gunn M, Meyers G. 2001. A family of closely related bovine viral diarrhoea virus recombinants identified in an animal suffering from mucosal disease: new insights into the development of a lethal disease in cattle. *Virology* 291:77–90. <https://doi.org/10.1006/viro.2001.1170>.
  59. Zou X, Zhu Y, Bao H, Guo X, Sun P, Liu Z, Mason PW, Xu L, Li C, Zhang Q, Wang Q, Zhu H, Zhao Q. 2019. Recombination of host cell mRNA with the Asia 1 foot-and-mouth disease virus genome in cell suspension culture. *Arch Virol* 164:41–50. <https://doi.org/10.1007/s00705-018-4008-2>.
  60. Ho SN, Hunt HD, Horton RM, Pullen JK, Pease LR. 1989. Site-directed mutagenesis by overlap extension using the polymerase chain reaction. *Gene* 77:51–59. [https://doi.org/10.1016/0378-1119\(89\)90358-2](https://doi.org/10.1016/0378-1119(89)90358-2).
  61. Reed LJ, Muench H. 1938. A simple method of estimating fifty per cent endpoints. *Am J Epidemiol* 27:493–497. <https://doi.org/10.1093/oxfordjournals.aje.a118408>.
  62. Beaucourt S, Borderia AV, Coffey LL, Gnädig NF, Sanz-Ramos M, Beeharry Y, Vignuzzi M. 2011. Isolation of fidelity variants of RNA viruses and characterization of virus mutation frequency. *J Vis Exp* 52:e2953. <https://doi.org/10.3791/2953>.